

Power Limits with Adjustable 10G Receiver Parameters for A-RoF Transmission

Inna Kurbatska^{1,*}, Armands Ostrovskis^{1,2}, Laura Skladova^{1,2}, Kristaps Rubuls², Sandis Spolitis^{1,2}, Vjaceslavs Bobrovs¹

¹*Institute of Telecommunications, Riga Technical University,
Azenes St. 12, LV-1048, Riga, Latvia*

²*Communication Technologies Research Center, Riga Technical University,
Azenes St. 12, LV-1048, Riga, Latvia*

*inna.kurbatska@gmail.com; armands.ostrovskis@rtu.lv; laura.skladova@rtu.lv;
kristaps.rubuls@rtu.lv; *sandis.spolitis@rtu.lv; vjaceslavs.bobrovs@rtu.lv*

Abstract—The current paper characterises the performance of the three radio frequency channels, orthogonal frequency division multiplexed (OFDM) radio-over-fiber (RoF) transmission system in terms of error vector magnitude and received optical signal power for a typical 10 GHz receiver obtained by the comprehensive simulations. The impact of the signal-to-noise ratio (SNR) of the OFDM channels transmitted is also considered. We demonstrate that the SNR decrease from 40 dB to 25 dB results in an error vector magnitude (EVM) increase of up to 4 %. Furthermore, we propose the approach to allow one to adjust these results to other receiver sensitivity and responsivity values by introducing a delta in received optical signal power, eliminating additional simulation or complicated calculations. The feasibility of adjustments with a precision of up to 0.001 % of the EVM is proved.

Index Terms—Radio-over-fiber; OFDM; Simulation; Optical receivers.

I. INTRODUCTION

With the rapid deployment of 5G underway, research has turned its focus toward defining the vision and technologies for 6G and working to enable even new indoor and outdoor services for operators to offer to customers [1]. Thus, the further development of radio-over-fiber (RoF) technologies is becoming crucial. Several solutions are being considered to meet the performance requirements of 6G [1]. Thus, reliable and effective mathematical simulations of RoF transmission systems, such as the one we provide in current research, are becoming a powerful tool for evaluating and developing new technologies.

One of the significant issues for researchers regarding the orthogonal frequency division multiplexed (OFDM) RoF transmission system is the trade-off between signal power and noise. For example, authors in [2] analyse the

theoretical perspective of improved receivers for OFDM regarding the optical signal-to-noise ratio (OSNR), and the authors in [3] focus on developing a transmitter with an improved SNR. Moreover, the authors in [4] utilise SNR for performance evaluation in the experimental investigation of the Mach-Zehnder modulator (MZM) for 32-quadrature amplitude modulated (QAM) OFDM. Furthermore, our previous research [5] has also shown that the OFDM RoF integrated into a passive optical network (PON) is loss-limited. Namely, noise has a critical impact on the performance of the OFDM RoF transmission system. It is also essential that several recently proposed realisations of RoF transmission systems utilise the multi-radio frequency (RF) channel transmission, e.g., in [6]–[10], which must also be considered. We focus on the intermediate frequency (IF) over fiber transmission with RF frequencies up to 10 GHz. This solution allows the integration of the RoF into the typical widely implemented PON architecture with 10 GHz transceivers and is widely used in recent research [6]–[9]. The possible solution to integrate sub-6 GHz RoF into PON architecture is demonstrated in [10]. The authors realise the transmission of the two OFDM signals with 16-QAM signals (at 1.5 GHz and 3.5 GHz, respectively) and one wired PON signal at 2.5 GHz. Thus, the transmission of the three RF channels on one optical carrier is realised. Our utilised architecture has three OFDM signals with 64-QAM signals spaced at 3.0 GHz, 3.5 GHz, and 4.0 GHz. Here, it is essential to mention that the researches in [6], [8], [10] aim at the demonstration of the feasibility of the new architectures, while the authors in [7] demonstrate the development of the transmitter. On the contrary, our research aims to develop a new approach for simulations to evaluate the power limits for different OFDM RoF transmission systems. Here, we demonstrate the utilisation of our approach and prove its feasibility by obtaining the power limits for the practically easy-implementable and potentially widespread architecture.

The current research focusses on obtaining the widely applicable limits in terms of error vector magnitude (EVM) and received optical signal power (ROP) in dependence on sensitivity (which characterises the noise of the PIN

Manuscript received 28 November, 2022; accepted 13 March, 2023.

This work has been supported by the European Regional Development Fund within the Activity 1.1.1.2 “Post-doctoral Research Aid” of the Specific Aid Objective 1.1.1 “To increase the research and innovative capacity of scientific institutions of Latvia and the ability to attract external financing, investing in human resources and infrastructure” of the Operational Programme “Growth and Employment” under Grant No. 1.1.1.2/VIAA/3/19/406, and in part by the Doctoral Grant programme of Riga Technical University in Latvia.

photodiode) for the multi-RF channel transmission system integrated into the PON. In such a way, we not only evaluate the performance and limits of the investigated multi-channel OFDM RoF transmission system utilisable for the design, further development, and standardisation. We also describe the approach to ensure the time efficiency of the simulation and extend the usability of the results provided. Namely, we provide the EVM dependence on the ROP for typical 10G RX. However, our developed and evaluated approach allows us to recalculate this EVM versus ROP curve for other receiver sensitivity and responsivity only by introducing an additional power penalty without other simulations or complicated calculations.

Previously, we have worked on the approach for the simulation of the thermal noise and received optical signal power, allowing us to adapt the simulation results for different power budgets, signal quality thresholds, and sensitivities without any additional simulation required. Here, we further improve the accessibility and usability of the results by providing the initial results in terms of sensitivity (instead of thermal noise), making the results quickly related to the technical specifications of the receivers. Moreover, the results can be easily adjusted to the receiver sensitivity and responsivity changes without additional simulations or complicated recalculations. In addition, in current research, we also cover the impact of transmitter noise by providing EVM versus ROP limits for different values of the SNR of the electrical OFDM signal to be transmitted.

II. SIMULATION SETUP AND METHODOLOGY

Figure 1 shows our developed simulation setup for a three RF channel OFDM RoF transmission system for a sub-6 GHz frequency range integrated into the PON architecture. The simulations are performed in the *VPI Design Suite* simulation software.

The parameters of the OFDM signal are chosen to be close to the 5G new radio (NR) signal parameters and satisfy the requirements of the simulation software for the efficient fast Fourier transform. Respectively, the typical sub-carrier spacing for a 5G NR signal is 240 kHz with a maximal number of sub-carriers of 3300. However, the high number of sub-carriers would set very high requirements for the memory of the hardware utilised for simulation. Furthermore, analysing the number of carriers used in scientific publications on the OFDM RoF implementation, the number of sub-carriers has typically varied from 800 to 2048, e.g., in [9], [11], [12]. For our setup, we have chosen the middle value of 1200 sub-carriers utilised in [12]. However, to ensure the efficient simulation in *VPI Design Suite* by providing that the great prime factor limit of the number of samples for fast Fourier transform will not increase 5, it has been required to choose the number of carriers corresponding to the power of 2. As a result, the final number of sub-carriers has been set to 1024, which for typical 240 kHz channel spacing would result in the baudrate of 245.76 MBaud. However, again addressing the requirement of *VPI Design Suite* to ensure an integer number of samples, and thus integer baudrate, it has been rounded to 250 MBaud.

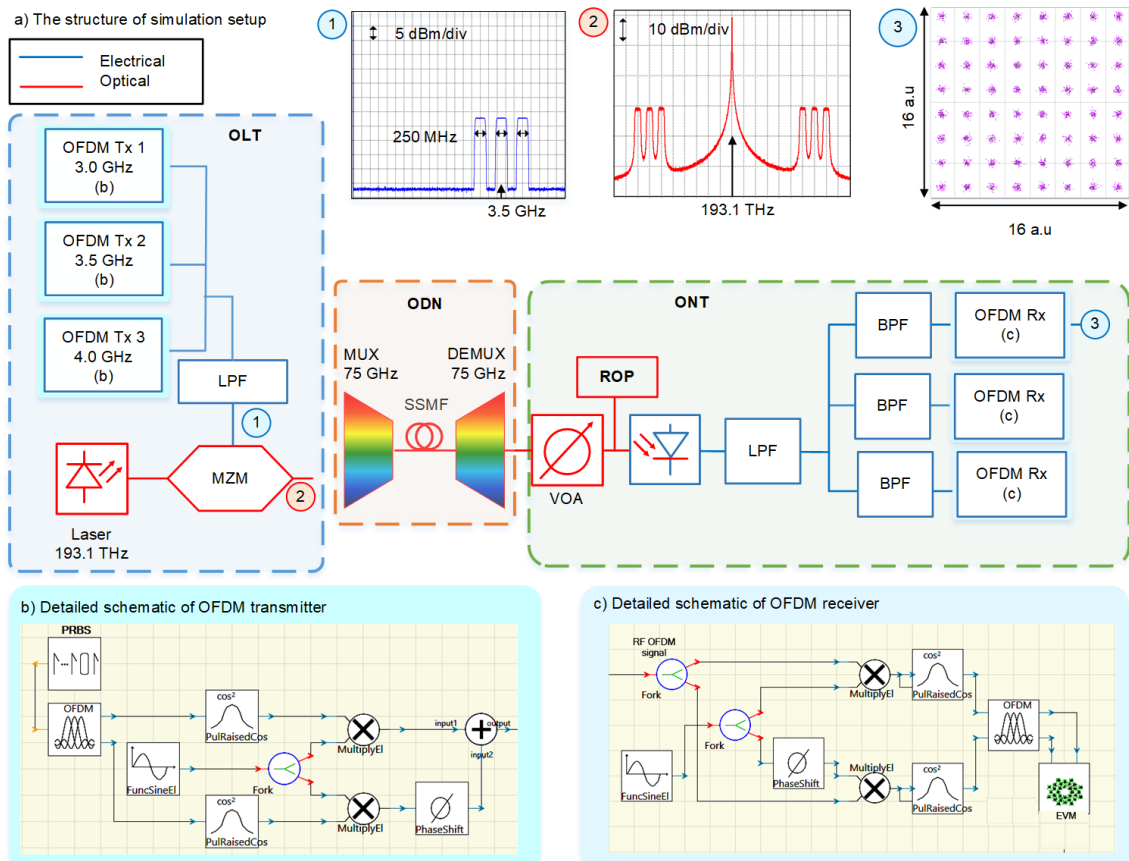


Fig. 1. The simulation setup of a three RF channel OFDM RoF transmission system for a sub-6 GHz frequency range integrated into the PON architecture: (a) The structure of simulation setup; (b) Detailed schematic of OFDM transmitter; (c) Detailed schematic of OFDM receiver.

The baudrate of 250 MBaud with 64-QAM corresponds to 1.5 Gbit/s per channel, resulting in a capacity of 4.5 Gbit/s for three channels. RF channels are spaced at 500 MHz at 3 GHz, 3.5 GHz, and 4 GHz. It is essential to mention that our goal in the current research was to consider possible interchannel interactions. Three RF channels are enough for this, as interchannel distortions are typically caused by adjacent channels. However, increasing the number of channels can increase the capacity of the system. But additional research is needed on the possible impact of the increased number of RF channels on the modulation.

The optical line terminal (OLT) consists of a continuous wave laser (corresponding to *CoBrite DXI* technical specification) with a frequency of 193.1 THz and minimal output power of 6 dBm. It is modulated by three combined OFDM channels utilising a Mach-Zehnder modulator (MZM) with an insertion loss of 4 dB and an extinction ratio of 20 dB (corresponding to the *Photline MX-LN-40* technical specification). The driving voltage of the MZM has been set to 7 V with the application of a bias voltage of 3.5 V to both arms of the MZM to ensure the simulation of a balanced single-drive MZM configuration. These parameters, together with adjusting the amplitude of the OFDM signal, also ensure the minimisation of the distortions in the modulation process that, according to our performed pre-research, may appear due to applying several RF channels.

The optical distribution network (ODN) comprises a 75 GHz multiplexer, demultiplexer, and standard single-mode fiber (SSMF) with an attenuation of 0.2 dB/km and a dispersion of 18 ps/nm/km, which is typical for C-band transmission.

The optical network terminal (ONT) consists of a standard 10 GHz PIN photoreceiver with a sensitivity of -19 dBm and a responsivity of 0.7 A/W, bandpass filters (BPFs) for selecting RF channels, and an OFDM receiver for the decoding and quality evaluation. 4-pole Bessel filters (LPFs) are utilised to simulate the bandwidth of the MZM and PIN photoreceiver. We used a variable optical attenuator (VOA) to adjust the ROP.

For the evaluation of the signal quality, we utilise error vector magnitude (EVM) described by (1) [13], [14]

$$EVM = \sqrt{\frac{\sum_{i=1}^{N_s} |IQ - IQ_{tx}|^2}{\sum_{i=1}^{N_s} |IQ_{tx}|^2}}, \quad (1)$$

where N_s is the number of complex symbols, IQ are the complex symbols received, but IQ_{tx} are the complex symbols transmitted [12]. In the simulation setup, the EVM is calculated for each OFDM sub-carrier, while we utilise the EVM value for the worst sub-carrier for the analysis.

There are two leading global parameters in the *VPI Photonics Design Suite* - the time window and sampling rate. These parameters determine the speed and precision of the simulation. Specifically, the optical signal is simulated as a complex time-dependent amplitude envelope of the optical field with carrier frequency as a parameter [13]. As the envelope is an analogue signal, it has to be sampled with the determined sampling rate for simulation purposes. Thus, the higher is frequency, the wider the simulated spectrum,

and the higher the precision. However, that also means a higher number of samples per bit, and thus a longer simulation time. At the same time, the time window parameter determines the number of simulated bits. The higher the number of bits, the higher precision of the signal quality evaluation that can be ensured. However, this also increases simulation time and requires high computational capacity, especially for a signal with a high number of samples. This trade-off between precision and time is vital for RoF transmission systems because these systems have a low symbol rate.

For the typical value of 16 samples per symbol, the sample rate (and thus the simulated RF bandwidth) for 250 Gbaud data rate would be 4 GHz, which is smaller than the Nyquist frequency for the 3.5 GHz RF carrier frequency. Addressing this, we utilise 128 samples per symbol. However, for this case, the maximum number of simulated symbols per sub-carrier that can be supported by software and hardware is 32. Nevertheless, it is not enough for a reliable estimation of the EVM. We overcome this problem by running several simulation runs with the accumulating EVM results per each run. The 20 runs resulting in 640 symbols per carrier have demonstrated to be sufficient to ensure precise EVM estimation (the EVM has not changed significantly with the further increase of the number of runs). Addressing this, we utilised 20 runs for the simulations in the scope of current research.

For our non-amplified, loss-limited transmission system, the thermal noise of the PIN photodiode is the main performance-affecting factor. In *VPI Design Suite*, this noise is considered by specifying the parameter thermal noise that defines the one-sided spectral noise density N_{th} , from now on thermal noise, measured in $[A/Hz^{1/2}]$ [13]. To relate thermal noise to the sensitivity parameter, widely available in the technical specifications of photoreceivers, we use (2) [15]

$$P_{pin} = Q\sqrt{S_T \times BW} / R, \quad (2)$$

where Q is the Q factor (corresponding to specific bit error rate (BER) for which the sensitivity is given in the specifications, R is the responsivity $[A/W]$, S_T is the spectral density of the thermal noise $[A^2/Hz]$, which is the square of the thermal noise N_{th} , but BW is a bandwidth of -3 dB of the receiver $[Hz]$ [15].

Previously, by investigating the relations among thermal noise, ROP, and calculated sensitivity, we have proved that the impact on performance has only a delta between ROP and sensitivity. As a result, we have developed the approach for calculating the EVM versus ROP or minimal required ROP versus thermal noise curves for different conditions, including a change of the responsivity utilising one simulated EVM versus thermal noise curve. It has been realised using *Matlab* and is approved by simulations. In the current research, we further improve the accessibility and usability of this approach.

In current research, we provide power limits for our investigated system in terms of EVM versus ROP, ensuring a comprehensive performance characterisation. Simulated results are provided for typical sensitivity values (-19 dBm)

and responsivity (0.7 A/W) for the 10 GHz receiver. However, they can be adjusted to other receiver sensitivity and responsivity values by simply introducing a delta in the ROP, eliminating complicated calculations. In addition, in current research, we also cover the impact of transmitter noise by providing EVM versus ROP limits for different values of the SNR of the electrical OFDM signal to be transmitted.

III. RESULTS AND DISCUSSION

This section provides the EVM dependence on the ROP (combining all the loss sources of the system) for a three RF channel OFDM RoF transmission system that utilises the 10G PIN receiver. The results are provided for different values of SNR (from 25 dB to 40 dB) of the RF signal to be transmitted. Moreover, the approach that allows adjustment of the obtained EVM versus ROP curve for other values of sensitivity and responsivity is described, demonstrated, and approved by simulations.

As the first step to the simulation efficiency and usability of the results, we have evaluated the feasibility of simulation of the loss of different sources (multiplexer and demultiplexer insertion loss, fiber attenuation, and the decrease of laser output power) by rearranging it in ROP. It is significant because in such a way the results can be applied to different PONs (different split ratios, types of splitter and combiners, types of fiber).

For this purpose, we have compared two ways of varying optical power - before and after ODN (blue, dotted lines in Fig. 2 and red, solid lines in Fig. 2, respectively). The optical power before ODN has been varied by adjusting the laser output power and also setting the typical fiber attenuation of 0.2 dB/km. Next, the corresponding ROP has been adjusted utilising VOA immediately after the ODN (before the receiver) without considering any other loss sources. As shown in Fig. 2, the difference in EVM is negligible. Thus, simulations can be performed only by varying the ROP. The multiplexer and demultiplexer insertion losses here have not been considered separately as it is also related to the change of the power before and after optical fiber that, as shown in Fig. 2, has an equal impact on the EVM.

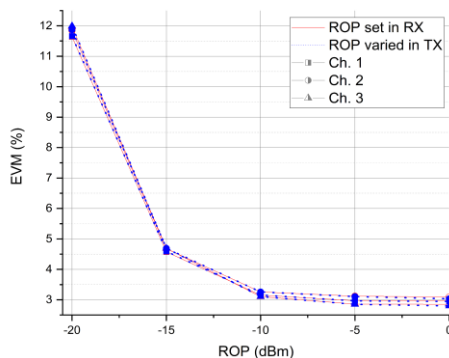


Fig. 2. Comparison of the optical power variations before (blue, dotted lines with solid symbols) and after (red, solid lines with open symbols) optical distribution network.

Considering the obtained results, we have continued with the minimal transmitter output power for our simulation setup (laser output power of 6 dBm according to the

technical specification and none of the amplification). As the insured ROP, in this case, is close to -10 dBm, the initial ROP has been fixed to -10 dBm, and further, it has been varied utilising VOA before the receiver.

Our previous investigations have been related to receiver noise. At the same time, noise in the modulator driving circuit can also significantly influence performance, as shown, e.g., in [3], [4]. In the current research, we are considering the impact of the SNR of the OFDM signal to be transmitted. We simulate noise in the transmitter utilising the electrical amplifier without gain to ensure the varying of SNR of the OFDM signal from 25 dB to 40 dB with the step of 5 dB. The 40 dB value has been chosen as a typical value for a good quality radio signal, while 25 dB was the minimal value of SNR capable of ensuring EVM below 8 %.

Figure 3(a) shows the EVM versus ROP curve for the different SNR values in the transmitter and the typical sensitivity (-19 dBm) and responsivity (0.7 A/W) for the 10 GHz receiver.

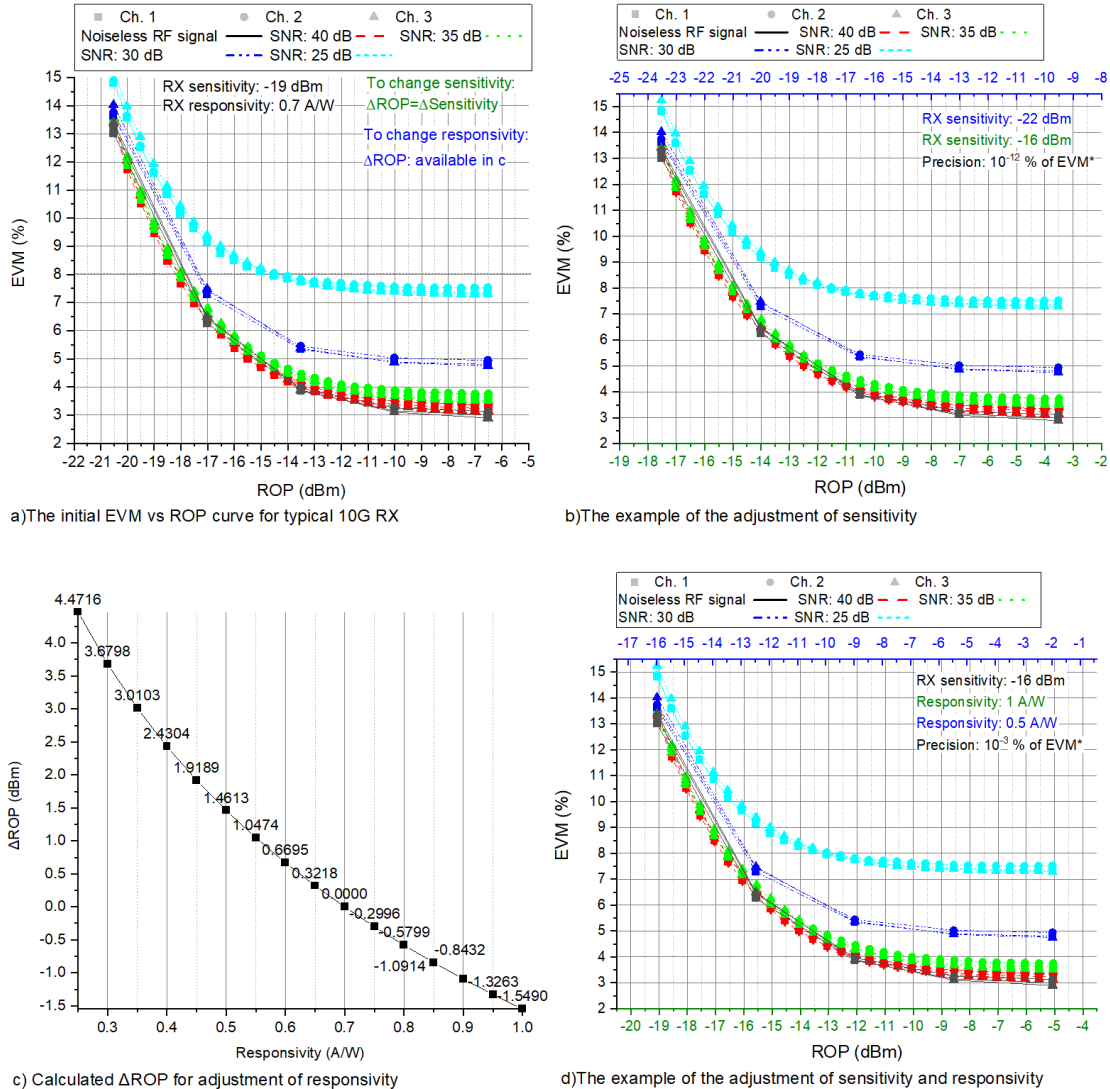
As shown in Fig. 3, the significant impact of interchannel interference has not been observed for our utilised channel spacing of 500 MHz. Respectively, the difference in EVM between the 1st, 2nd, and 3rd channels (square, circle, and triangle in Fig. 3) is not significant. Considering that interchannel interference is typically caused by adjacent channels, it is possible to conclude that there is no significant interchannel interference for the multi-RF channel transmission system. However, it is necessary to mention that during our research, the distortions in the modulation process have been observed due to the application of several RF channels. To eliminate this impact, the parameters of the MZM driving circuit had to be adjusted. However, this is specific to the different modulation techniques and transmitters, so it may be addressed in separate future research. The current study assumes that the performance evaluation stage already resolves modulation issues (like in the current research).

As shown in Fig. 3(a), the impact of the transmitted signal SNR is non-linear. For relatively high SNR (above 35 dB), the difference in EVM compared to a noiseless signal is below 1 % of EVM. On the contrary, the decrease in SNR from 35 dB to 30 dB and 30 dB to 25 dB results in an increase in EVM of 1.2 % and 2.6 %. Consequently, the impact of the SNR of the OFDM signal to be transmitted is crucial (the decrease of SNR from 40 dB to 25 dB results in the an increase in the EVM of 4.2 %). We can also observe that the curves obtained for 30 dB and 25 dB become steady for the ROP increase from -10 dBm to -6.5 dBm. Consequently, the low SNR in the transmitter cannot be compensated for by an increase in ROP. Therefore, the impact of the SNR of the transmitter must be considered separately.

As we can see in Fig. 3(a), for our simulated OFDM RoF transmission system, the minimal EVM that is possible to ensure with the increase of ROP for SNR above 35 dB is below 4 %, for 30 dB - below 5 %, and only about 7.5 % for the SNR of 25 dB. Thus, it is possible to conclude that the acceptable SNR is above 30 dB. Furthermore, the ROP required to ensure that the EVM threshold of 8 % is similar

(up to -18 dBm) for the SNR of above 35 dB, the increase of SNR to 30 dB requires an increase of ROP for about 0.7 dB, while the rise of SNR to 25 dB - by 3.5 dB. It is essential to mention that the threshold of 8% is chosen following the typical requirements for the 5G NR signal. However, in our case, the threshold is used only for the impact analysis, as the impact of radio transmission is

outside the scope of current research. So, another quality threshold may be required for RoF transmission, depending on the quality of the wireless transmission. This is one of the reasons for our efforts in providing widely applicable results that can be utilised for different conditions, including different EVM requirements.



*precision depends on the precision of the ROP and thermal noise set for simulation

Fig. 3. Dependence of the EVM on the ROP, which combines all the loss sources of the system obtained for the three RF channel OFDM RoF transmission system with a 10G PIN receiver: (a) The initial EVM vs. ROP curve for typical 10G RX; (b) The example of the adjustment of sensitivity; (c) Calculated Δ ROP for adjustment of responsivity; (d) The example of the adjustment of sensitivity and responsivity.

At the next research stage, the feasibility of adjusting the obtained EVM versus ROP curve to other parameters of the 10G transmitter has been proposed and approved. To adjust the results provided in Fig. 3(a) to other receiver sensitivity and responsivity values, we introduce Δ ROP. As we have proved in our previous research [16], the sensitivity change can be compensated for by the exact change of the ROP. Therefore, to adjust the EVM versus ROP curve for another sensitivity, it is necessary to change the ROP by the same Δ .

Fig 3(b) shows an example of the adjustment of sensitivity to -22 dBm by applying Δ ROP of -3 dB (blue, upper x-axis) and -16 dBm by using Δ ROP of 3 dB (green, lower x-axis). The adjusted results have also been approved by simulations, and the same EVM values with precision

greater than 1×10^{-12} % have been obtained. In this case, the accuracy depends on the precision of thermal noise (12 decimal digits have been utilised) and ROP (4 decimal digits) set in simulation software.

Fig. 3(c) provides our calculated values of the Δ ROP for different responsivity, which is necessary to apply for Fig. 3(a), to adjust the ROP values for another responsivity. The delta values have been calculated as follows. The new responsivity value is put in (2) and the sensitivity value corresponding to this new responsivity is calculated. In this case, the delta ROP is the delta between this newly calculated sensitivity and the previously utilised. Actually, the change in responsivity is related to the corresponding change in sensitivity. The delta ROP given in Fig. 3(c) with

a precision of 4 decimal digits is sufficient to ensure the accuracy of the adjustment of 1×10^{-3} % of EVM.

Figure 3(d) shows the example of adjusting responsivity to 1 (green, lower x-axis) and 0.5 A/W (blue, upper x-axis) by applying the Δ ROP of -1.5490 dB and 1.4613 dB. Moreover, the responsivity adjustment is performed on the already adjusted sensitivity of -16 dBm (with the applied delta ROP of 3 dB), demonstrating the feasibility of simultaneous adjustment. These results have also been approved by simulations. Due to the necessity of calculations, the precision of the EVM ensured, in this case, is smaller, up to 1×10^{-3} % of the EVM, provided by the thermal noise precision of 12 decimal digits and the ROP of 4 decimal digits. However, this precision is still more than enough for signal quality evaluation in terms of EVM.

IV. CONCLUSIONS

In the current research, we have investigated the evaluation of performance limits in terms of EVM and ROP for a three RF channel OFDM RoF transmission system with a 10G PIN receiver. We have proved that it is feasible to ensure a similar EVM using ROP to characterise the whole power budget of the system without distinguishing separate optical signal loss sources. We have also confirmed that there is no significant impact of interchannel interference (the difference in EVM among channels does not exceed 0.5 %) for our investigated channel spacing of 500 MHz.

We have also investigated the impact of the SNR of the OFDM signal to be transmitted. As a result, we have demonstrated that the impact of the SNR of the OFDM signal to be transmitted is crucial (the decrease of SNR from 40 dB to 25 dB results in an increase in EVM of 4.2 %). It is also non-linear and cannot be compensated for with increased ROP. The acceptable SNR is above 30 dB (less than 1 dB ROP increase is required to ensure EVM of 8 %), while the rise of SNR to 25 dB requires a significant ROP increase (about 3.5 dB to ensure EVM of 8 %). The minimal EVM can be provided with the increase of ROP for SNR above 35 dB being below 4 %, for 30 dB being below 5 %, and only about 7.5 % for the SNR of 25 dB.

We have also proposed, demonstrated, and evaluated by approving the calculated results with simulations an approach allowing us to adjust the obtained ROP limits for sensitivity and responsivity of other 10G PIN photoreceivers without additional simulations and complicated calculations, ensuring the precision up to 0.001 % of EVM. In such a way, we combine the physical parameter thermal noise, the sensitivity parameter from technical specifications, and the measurable parameter ROP, as well as increasing time efficiency and ensuring the usability of the results, which can be adjusted without specific software.

CONFLICTS OF INTEREST

The authors declare that they have no conflicts of interest.

REFERENCES

- [1] T. Sizer *et al.*, "Integrated solutions for deployment of 6G mobile networks", *Journal of Lightwave Technology*, vol. 40, no. 2, pp. 346–357, 2022. DOI: 10.1109/JLT.2021.3110436.
- [2] X. Liu, J. Zhou, N. Huang, and W. Zhang, "Improved receivers for optical wireless OFDM: An information theoretic perspective", *IEEE Transactions on Communications*, vol. 70, no. 7, pp. 4439–4453, 2022. DOI: 10.1109/TCOMM.2022.3174102.
- [3] L. Zhong *et al.*, "An SNR-improved transmitter of delta-sigma modulation supported ultra-high-order QAM signal for fronthaul/WiFi applications", *Journal of Lightwave Technology*, vol. 40, no. 9, pp. 2780–2790, 2022. DOI: 10.1109/JLT.2022.3147059.
- [4] S.-C. Kao, K.-F. Chung, C.-T. Tsai, D.-W. Huang, T.-T. Shih, and G.-R. Lin "High-baud-rate 32-QAM OFDM single-arm and dual-arm encoded silicon Mach-Zehnder modulator", in *Proc. of 2021 30th Wireless and Optical Communications Conf.*, 2021, pp. 46–48. DOI: 10.1109/WOCC53213.2021.9603131.
- [5] I. Kurbatska, S. Spolitis, and V. Bobrovs, "Evaluation of the performance-affecting factors in the converged PON", in *Proc. of 2021 25th International Conf. Electronics*, 2021, pp. 1–6. DOI: 10.1109/IEECONF52705.2021.9467482.
- [6] C. H. de Souza Lopes, E. S. Lima, L. A. Melo Pereira, and A. C. Sodré, "Peaceful coexistence between 5G NR and LTE-A over a RoF-based fronthaul", in *Proc. of 2021 SBFoton International Optics and Photonics Conf.*, 2021, pp. 1–4. DOI: 10.1109/SBFotonIOPC50774.2021.9461959.
- [7] M. T. Milojkovic, A. D. Djordjevic, S. L. Peric, M. B. Milovanovic, Z. H. Peric, and N. B. Dankovic, "Model Predictive Control of Nonlinear MIMO Systems Based on Adaptive Orthogonal Polynomial Networks", *Elektron Elektrotech*, vol. 27, no. 2, pp. 4–10, Apr. 2021. DOI: 10.5755/j02.eie.28780.
- [8] K. Tanaka *et al.*, "1.314-Tbit/s (576 × 380.16-MHz 5G NR OFDM signals) SDM/WDM/SCM-based IF-over-fiber transmission for analog mobile fronthaul", in *Proc. of 2022 Optical Fiber Communications Conf. and Exhibition*, 2022, pp. 1–3. DOI: 10.1364/OFC.2022.W4C.2.
- [9] S. Shen, T. Zhang, S. Mao, and G.-K. Chang, "DRL-based channel and latency aware radio resource allocation for 5G service-oriented RoF-mmWave RAN", *Journal of Lightwave Technology*, vol. 39, no. 18, pp. 5706–5714, 2021. DOI: 10.1109/JLT.2021.3093760.
- [10] T. H. Dahawi, Z. Yusoff, M. S. Salleh, and J. M. Senior, "Low-cost MIMO-RoF-PON architecture for next-generation integrated wired and wireless access networks", *Journal of Optical Communications and Networking*, vol. 13, no. 3, pp. 41–52, 2021. DOI: 10.1364/JOCN.413596.
- [11] L. A. Neto *et al.*, "Experimental demonstration of A-RoF SDN for network sharing applications", in *Proc. of 2020 Optical Fiber Communications Conf. and Exhibition (OFC)*, 2020, pp. 1–3. DOI: 10.1364/OFC.2020.T4A.4.
- [12] S. Yao *et al.*, "Non-orthogonal uplink services through co-transport of D-RoF/A-RoF in mobile fronthaul", *Journal of Lightwave Technology*, vol. 38, no. 14, pp. 3637–3643, 2020. DOI: 10.1109/JLT.2020.2980208.
- [13] *Photonic modules*. Documentation of VPI Design Suite by VPIPhotonics GmbH, 2022.
- [14] *IEEE standards*. IEEE 802.11.a standardization (ISO/IEC 8802-11:1999/Amd 1:2000(E)), Release 1:83, 1999.
- [15] G. P. Agrawal, *Fiber-Optic Communications Systems*, 3rd ed. Wiley, Rochester (NY), 2002. DOI: 10.1002/0471221147.
- [16] I. Kurbatska, S. Spolitis, and V. Bobrovs, "The investigation on the modeling of the receiver sensitivity in the RoF transmission systems", in *Proc. of 2021 Photonics & Electromagnetics Research Symposium (PIERS)*, 2021, pp. 1020–1025. DOI: 10.1109/PIERS53385.2021.9694696.



This article is an open access article distributed under the terms and conditions of the Creative Commons Attribution 4.0 (CC BY 4.0) license (<http://creativecommons.org/licenses/by/4.0/>).